Towards Automated Detection of Rheumatic Heart Disease Using Classical Computer Vision Techniques

Naila Suele Mascarenhas Silva*, Carlos Alberto Rodrigues*, Airandes de Sousa Pinto†,
Bráulio Muzzi Ribeiro de Oliveira‡, Renata Fonseca Mendoza† and Maria do Carmo Pereira Nunes§
*Departamento de Ciências Exatas, Universidade Estadual de Feira de Santana, BA, Brasil
†Departamento de Saúde, Universidade Estadual de Feira de Santana, BA, Brasil
‡Instituto de Previdência dos Servidores do Estado de Minas Gerais - IPSEMG, Belo Horizonte, MG, Brasil
§Faculdade de Medicina, Universidade Federal de Minas Gerais, Belo Horizonte, MG, Brasil
E-mail: nailasuely@ecomp.uefs.br, carod@uefs.br

***Abstract*—Acute Rheumatic Fever (ARF) and its primary sequela, Chronic Rheumatic Heart Disease (RHD), remain a significant public health problem, particularly in developing countries. Early diagnosis of RHD, based on echocardiographic criteria such as anterior mitral leaflet (AML) thickening, is crucial for preventing disease progression. However, manual assessment of these parameters is subjective, time-consuming, and limited by the inherently noisy quality of echocardiography images. This study proposes and validates the tip-to-base thickness ratio as a quantitative biomarker, derived from a semi-automated, interpretable pipeline for assessing AML thickening. The methodology encompasses leaflet segmentation through Otsu's thresholding and morphological operations, followed by the extraction of its medial axis and division into anatomically relevant segments (base, middle, and tip). Validating on a dataset of 80 pediatric echocardiograms (17 ARF, 63 controls), our results indicate that the proposed tip-to-base thickness ratio was significantly higher in patients with ARF ($p = 0.03$), yielding an Area Under the Curve (AUC) of 0.67 for disease classification. By providing a fully transparent and reproducible measurement, this work demonstrates the feasibility of using classic computational methods to create objective tools for RHD screening, highlighting the value of interpretable classical methods for clinical decision support in RHD screening.**

I. Introduction

Acute Rheumatic Fever (ARF) is an inflammatory syndrome that occurs as a late sequela of group A *Streptococcus* infection, primarily affecting children and young adults in low-resource settings where access to diagnosis and treatment is inadequate [1]. Among the most severe manifestations of ARF is carditis, which can progress to Chronic Rheumatic Heart Disease (RHD) [2]. RHD is recognized as the leading cause of acquired cardiovascular morbidity and mortality in the young population, with a global impact estimated at over 300,000 deaths annually. In Brazil, despite a downward trend in incidence, the prevalence of RHD and its associated mortality remain high, reflecting socioeconomic disparities and asymmetries in access to specialized care [3]. Recent data from the Hospital Information System (SIH/SUS) show a significant hospital burden related to RHD between 2020 and 2024, with a higher concentration in the Southeast and Northeast regions [4].

Early diagnosis of RHD is essential, as it enables secondary prophylaxis with benzathine penicillin, a low-cost and highly effective measure for preventing ARF recurrences and halting the progression of valvular disease [5]. The World Heart Federation (WHF) guidelines, updated in 2023, provide detailed echocardiographic criteria for diagnosing rheumatic heart involvement. Among the morphological findings, anterior mitral leaflet (AML) thickening is prominent, with well-established age-based parameters, such as a thickness threshold of ≥ 3.0 mm for individuals up to 20 years of age [6]. Values above this threshold, especially when associated with pathological mitral regurgitation, are indicative of rheumatic involvement. The precise detection of this thickening is crucial, as timely intervention can interrupt the progression to more severe forms of RHD, reducing the risk of complications such as significant valvular dysfunction, heart failure, and the need for surgery [5]. This underscores the clinical relevance of reliable diagnostic tools for assessing AML morphology.

Two-dimensional transthoracic echocardiography (TTE) remains the primary imaging modality for the diagnosis, monitoring, and assessment of ARF and its valvular manifestations. The parasternal long-axis (PLAX) view is frequently used to observe the thickness and mobility of the mitral leaflets [7]. However, this examination is highly operator-dependent, with variability in both image acquisition and interpretation. Furthermore, inherent imaging limitations such as speckle noise, anatomical artifacts, and acoustic shadowing can hinder the clear visualization of the leaflets [8]. This can compromise the accuracy of AML thickness measurements, increase inter-observer variability, and reduce the reliability of longitudinal assessments. Such limitations highlight the need for more standardized and objective methods to quantify anterior mitral valve thickening.

In this context, the application of computer vision and medical image analysis techniques represents a promising alternative to overcome the challenges of manual assessment.

Automated or semi-automated methods allow for objective, reproducible, and potentially more accurate quantification of valvular morphology, minimizing human subjectivity. These solutions can also facilitate the analysis of large volumes of echocardiographic images, with a positive impact on both research and clinical practice. Integrated into existing workflows, these tools have the potential to accelerate diagnosis and provide decision support based on quantitative data. With the advancement of portable echocardiography devices, the development of computational systems can expand access to specialized diagnosis, especially in regions endemic for RHD [9]. By democratizing specialized assessment, these technologies contribute to a more timely initiation of prophylaxis and, consequently, to reducing the impact of rheumatic heart disease in vulnerable populations.

Thus, this paper proposes and details the development of a semi-automated computational workflow for the objective quantification and segmentation of AML thickening from echocardiogram videos. The approach utilizes a sequence of classic image processing techniques, including Otsu's thresholding [10], mathematical morphology, and medial axis extraction, to analyze the leaflet's morphology in a reproducible manner. The main objective is to validate this method by investigating whether quantitative metrics derived from the algorithm, particularly the tip-to-base thickness ratio, can statistically differentiate a group of patients with acute rheumatic fever from a healthy control group. Unlike approaches based on convolutional neural networks (CNNs), which function as black boxes and require large volumes of labeled data [11], the proposal presented here is fully interpretable and adaptable to different anatomical variations. In this regard, we use morphological operations in conjunction with skeleton extraction, drawing inspiration from classic structural segmentation strategies applied to cardiac images, as proposed by Suri et al. [12], so that the leaflet can be segmented with anatomical precision. Otsu's method is adopted to separate relevant structures with computational simplicity and robustness to intensity variations, a significant advantage over deep learning-based methods. We show that it is possible to achieve promising results on an initial dataset of 17 cases of acute rheumatic fever and 63 controls, without the need for supervised training. This feasibility study serves as a first step towards validating the proposed biomarker, which will be further tested on an expanded dataset. The contributions of this work are as follows: (i) a semi-automated, transparent, and traceable pipeline for cardiac leaflet segmentation; (ii) a robust approach for small samples, with fine control over each step of the process; and (iii) a comparative statistical analysis that highlights leaflet thickening in cases of acute rheumatic fever.

The remainder of this paper is organized as follows: Section II reviews the relevant literature. Section III details the proposed method; Section IV presents the results, followed by the discussion in Section V; finally, Section VI presents the conclusions and suggestions for future work.

II. Related Work

The automated analysis of echocardiographic images is a growing field of research, driven by the need to reduce the subjectivity and inter-observer variability inherent in manual measurements [13]. The segmentation of cardiac structures, particularly of the mitral valve, is a critical step for quantitative assessment, but it is challenged by speckle noise, low contrast, and anatomical variability [8].

Deep learning, especially with the use of Convolutional Neural Networks (CNNs), has become the leading approach for many medical image segmentation tasks [11], [14]. Architectures like U-Net [15] are widely recognized for their effectiveness in biomedical imaging due to their ability to capture local and global context. Several studies have applied deep learning to automatically segment cardiac structures, including the mitral valve, with high accuracy [13], [16]. In a recent study directly related to RHD, Brown et al. [17] demonstrated a dual approach focusing on mitral regurgitation. They combined a classical machine learning model (a Support Vector Machine using 9 morphological and hemodynamic features of the regurgitant jet) with a more complex deep learning model (an ensemble of 3D CNNs and Transformers). Notably, their classical model achieved a higher Area Under the Curve (AUC) of 0.93 compared to the 0.84 from the deep learning approach [17]. However, these supervised and complex methods are heavily dependent on large, expertly annotated datasets, which are expensive and time-consuming to create. Furthermore, their "black-box" nature can make the results difficult to interpret, a significant drawback in clinical decision-making.

Before the dominance of deep learning, and still relevant for specific applications, a variety of semi-automated and classical image processing techniques were proposed. These methods include active contour models (or snakes) [18], level-set methods, and optimization-based approaches that evolve a curve to fit object contours. For instance, Kulkarni and Madathil [19] proposed an optimization-based algorithm using wavelet decomposition to segment the left ventricle, achieving a high Dice Coefficient of 0.9353 against ground truth labels. Similarly, Danilov et al. [20] developed an efficient workflow comparing various filtering and segmentation techniques for right heart analysis, identifying an optimal path that included a total variation filter and isoline delineation, which achieved the highest "Global Index" (a combined metric of speed and accuracy) of 0.90 among the tested segmentation methods. In the context of 3D echocardiography, Barros Filho et al. [21] used digital image processing to automatically measure the mitral valve area, with a Bland-Altman analysis showing high agreement with manual measurements, reflected in a maximal measurement difference of only 0.2 cm² for stenotic valves. These methods are often more interpretable, require less data, and can provide a reliable alternative when large annotated datasets are not available. Our work is situated within this context, leveraging a sequence of well-established and transparent image processing steps to create a reproducible and objective pipeline for quantifying AML morphology, a key indicator in RHD.

III. Methods

The echocardiogram videos that support the findings of this study are available from the corresponding author upon reasonable request. Data sharing will be considered on a case-by-case basis, in accordance with the study's ethical approvals.

A. Data Acquisition and Preparation

Two-dimensional echocardiographic data were collected from 80 pediatric patients at the Hospital da Criança in Feira de Santana, Bahia, Brazil. The study group consisted of 17 patients with a confirmed diagnosis of acute rheumatic fever, according to the revised Jones criteria [22], and a control group of 63 healthy individuals. All diagnoses were validated by a general committee of specialists. All examinations were acquired in digital format (AVI or MP4) for subsequent computational analysis.

The echocardiographic acquisitions were performed using standardized views, with a primary focus on the apical four-chamber and parasternal long-axis views, which optimize the visualization of the anterior mitral valve leaflet. The use of consistent views is important to ensure the compatibility and potential reproducibility of the measurements extracted by the algorithm. The videos were processed frame-by-frame, allowing for a detailed analysis of the entire cardiac cycle to identify morphological changes of interest.

B. Computational Methodology

The computational methodology developed for quantifying the thickness of the AML was implemented in Python, using the OpenCV [23] and Scikit-image [24] libraries. The process is structured as a sequential workflow that begins with manual intervention and proceeds with automated steps for segmentation, feature extraction, and measurement (Figure 1).

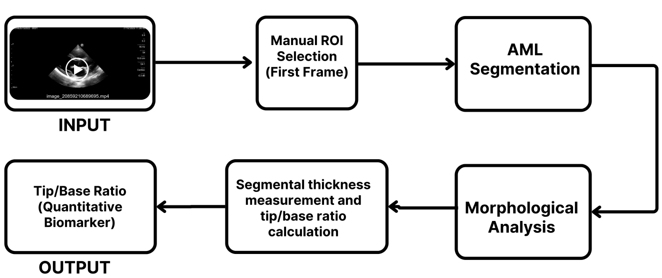

Fig. 1. Flowchart of the proposed computational pipeline for segmentation and quantification of AML morphology.

The process starts semi-automatically. An operator manually selects a rectangular Region of Interest (ROI) in the first frame of each echocardiogram video, encompassing the AML (Figure 2). This ROI defines the search area for subsequent processing in all frames of the video, ensuring that the algorithm focuses on the correct anatomical structure and reduces computational load.

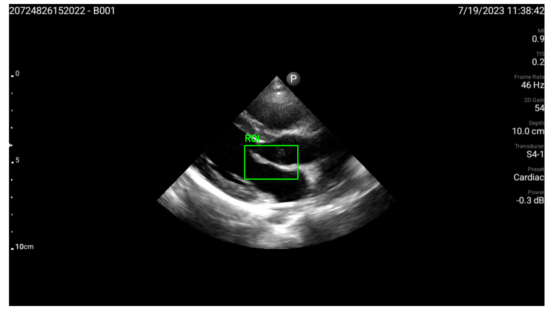

Fig. 2. Echocardiographic frame with manually selected Region of Interest (ROI) over the AML.

For each frame of the video, the sub-image within the ROI is subjected to a sequential segmentation workflow:

1) **Preprocessing and Binarization:** The image is converted to an 8-bit grayscale to standardize intensity analysis [25]. Then, Otsu's thresholding method is applied. This technique automatically calculates an optimal global intensity threshold that separates pixels into two classes (foreground/valvular tissue and background) by minimizing the intra-class variance [10], resulting in an initial binary mask of the leaflet.
2) **Morphological Refinement:** The initial binary mask is refined through sequential morphological operations to mitigate noise, such as speckle. First, a closing operation (dilation followed by erosion) with a 5×5 structuring element is used to fill small internal gaps in the leaflet and connect adjacent components. Subsequently, an opening operation (erosion followed by dilation) with the same structuring element is applied to remove small artifacts and smooth the leaflet's contours.
3) **Leaflet Isolation:** After refinement, the algorithm identifies all connected components in the image and retains only the largest one based on area. This assumes that the largest object within the ROI corresponds to the AML of interest (Figure 3).

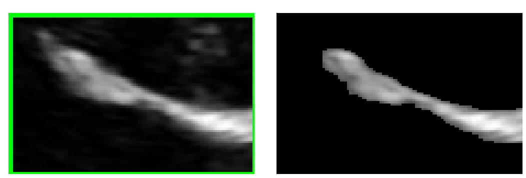

Fig. 3. Segmented AML within the ROI after binarization and morphological operations.

Quantitative Morphology Extraction and Analysis:

1) **Medial Axis Extraction (Skeletonization):** With the leaflet segmented, the medial axis transform (skeletonization) is applied to the binary mask to extract its skeleton—a one-pixel-thick centerline that is equidistant from the leaflet's contours. Before the transformation, a Gaussian filter is applied to smooth the mask, resulting in a more stable skeleton. The initial skeleton often

contains unnecessary branches; therefore, a pruning algorithm is applied iteratively to remove these artifacts, generating a clean and anatomically representative central axis (Figure 4A).

2) **Flexion Point Identification:** To divide the leaflet anatomically, a flexion point, corresponding to the region of maximum curvature, is automatically identified. The algorithm analyzes the leaflet's outer contour and estimates the curvature at each location by the angular variation between sets of three adjacent points. The point of greatest curvature is selected, with a refinement based on the minimum Euclidean distance to the leaflet's geometric center, ensuring a reliable segmentation landmark.
3) **Division into Segments:** Using the flexion point as a landmark, the leaflet's skeleton is divided into three contiguous, non-overlapping segments: base, middle, and tip (Figure 4B).

Quantitative Thickness Measurement:

1) **Thickness Calculation:** The leaflet's thickness is measured perpendicularly to the skeleton in each of the three segments. For each point along the skeleton, the thickness is calculated as twice the shortest Euclidean distance from that point to the contour of the segmented leaflet (Figure 5).
2) **Calibration and Aggregation:** The measurements, initially in pixels, are converted to millimeters using a single scale factor determined once for each video. This factor is established by measuring the length of the on-screen depth scale marker (in cm) in pixels using image editing software, which provides a precise pixels-per-millimeter ratio. For each frame, the algorithm measures thickness in pixels and applies this constant ratio to convert the values to millimeters. Finally, the segmental thickness values (mean and maximum) are calculated by aggregating the measurements from all analyzed frames for each patient, providing a comprehensive assessment throughout the cardiac cycle. Additionally, the tip-to-base thickness ratio is computed.

The Mann-Whitney U test was used to compare the groups. The accuracy of the tip-to-base thickness ratio for diagnosing acute rheumatic fever was evaluated using Receiver Operating Characteristic (ROC) curve analysis. Statistical significance was set at $p < 0.05$.

IV. Results

The study cohort comprised 17 patients with suspected ARF (Group 1) and 63 healthy controls (Group 2). The quantitative measurements derived from the algorithm, summarized in Table I, revealed that the tip-to-base thickness ratio of the AML was significantly higher in Group 1 (median: 1.04, IQR: 0.28) compared to Group 2 (median: 0.94, IQR: 0.18), with a *p*-value of 0.032 and a large effect size (Cohen's d = 0.76). Figure 6 visually illustrates the distribution of this metric and the difference between the groups. In contrast, the absolute thickness values for the base and middle segments did not reach statistical significance, although the tip segment exhibited a trend toward greater thickening in the patient group ($p = 0.074$).

TABLE I
Comparison of AML Measurements Between Groups

Variable	**Group 1 (Patients)** Median [IQR]	**Group 2 (Controls)** Median [IQR]	***p*-value**
Base (mm)	3.10 [1.18]	2.95 [0.87]	0.64
Middle (mm)	3.18 [1.09]	2.91 [0.79]	0.93
Tip (mm)	3.08 [1.04]	2.71 [0.70]	0.07
Tip/Base Ratio	**1.04 [0.28]**	**0.94 [0.18]**	**0.03**

IQR: Interquartile Range.

Frame-by-frame analysis across the cardiac cycle showed low intra-patient variability in thickness measurements (mean standard deviation < 0.25 mm per segment), indicating temporal stability and robustness of the proposed method. Calibration procedures ensured accurate conversion from pixels to millimeters, enabling reliable comparisons between individuals.

To evaluate the discriminative performance of the tip-to-base ratio, a Receiver Operating Characteristic (ROC) curve was generated, as shown in Figure 7. The analysis resulted in an Area Under the Curve (AUC) of 0.67 (95% confidence interval: 0.52–0.82). Using a threshold of 1.00 for the ratio yielded a sensitivity of 70.6% and specificity of 65.1%, suggesting the metric's potential as a quantitative biomarker for early-stage RHD detection in resource-constrained environments.

V. Discussion

The findings of this study demonstrate that the tip-to-base thickness ratio of the AML provides a statistically significant marker for distinguishing patients with ARF from healthy controls. This finding is clinically relevant, as the initial phase of rheumatic carditis is characterized by the formation of small verrucous nodules precisely along the valve coaptation lines (the leaflet tips) where mechanical stress is highest [26]. This process evolves into chronic, non-uniform fibrotic thickening. Our proposed tip-to-base ratio metric is therefore specifically designed to quantify this key pathological feature, unlike absolute segmental thickness values, which showed trends without reaching statistical significance. The relative nature of this ratio also appears to mitigate inter-individual variability in leaflet and heart dimensions.

In the clinical context, the value of this segmental analysis lies in its objectivity and reproducibility. Its interpretable nature, allowing clinicians to trace each processing step, is a key advantage for building clinical trust. While the resulting AUC of 0.67 is moderate, it is important to contextualize this performance against the literature. For example, the dual-approach study by Brown et al. [17] achieved an AUC of 0.93 for a classical model and 0.84 for a deep learning model. A key distinction, however, is that their method focused on analyzing

Fig. 4. (A) Segmented AML with overlay pruned medial axis (in blue). (B) Segmentation of the AML, base, middle and tip segments, guided by the flexion point (yellow circle) and shown along the skeleton (blue) with cyan division lines.

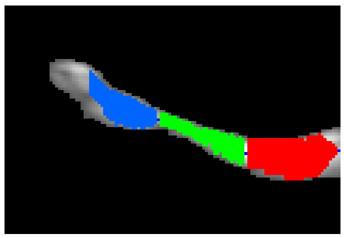

Fig. 5. Illustration of segmental thickness measurements (e.g., color-coded tip in light blue, middle in green, base in red).

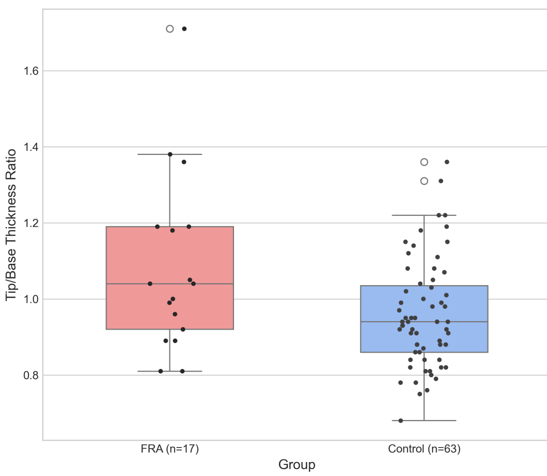

Fig. 6. Box plot comparing leaflet tip-to-base ratio between patients with suspected acute rheumatic fever (Group 1) and controls. The median was significantly higher in the patient group ($p = 0.03$).

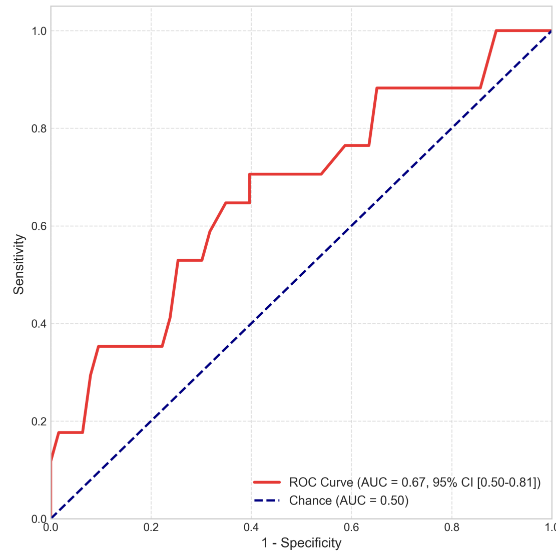

Fig. 7. Receiver Operating Characteristic (ROC) curve for predicting acute rheumatic fever. The Area Under the Curve (AUC) of 0.67 (IC 95%: 0.52–0.82) reflects the accuracy of the model to discriminate between predicting acute rheumatic fever and healthy. The dashed line represents the chance line (AUC=0.5).

features of the mitral regurgitation jet, while the present approach targets the direct morphological assessment of the leaflet tissue itself, representing a distinct and complementary diagnostic task. The segmentation strategy is also based on robust classical techniques that have demonstrated high accuracy in related contexts, such as Dice Coefficients above 0.93 [19] and high agreement in direct valve measurements [21], which supports the reliability of the underlying measurements.

This result must be viewed in light of the study's primary limitation: the small, imbalanced, single-center dataset. This dataset was used due to its specific focus on a pediatric population diagnosed under a consistent clinical protocol, and to the best of our knowledge, large-scale public datasets annotated for pediatric ARF are not readily available. Furthermore, the current pipeline relies on manual ROI selection, limiting full automation. It is also worth considering that the morphological refinement step, while necessary for noise removal, might result in a segmentation that is subtly thinner than the original structure; however, its impact on the relative tip-to-base ratio is likely minimal since this adjustment occurs homogeneously. A detailed sensitivity analysis of its parameters was also outside the scope of this preliminary work. Validating this method on larger, multi-center cohorts is an essential next step to confirm its generalizability and clinical utility.

Taken together, these results support the integration of relative morphometric indices, such as the tip-to-base ratio, into echocardiographic assessment protocols. They also motivate future work to explore their utility in longitudinal monitoring and early detection of RHD in endemic regions.

VI. Conclusion and Future Work

This work successfully demonstrated the feasibility of a semi-automated, structurally transparent pipeline for quantifying anterior mitral leaflet morphology. We proposed and validated the tip-to-base thickness ratio as a promising quantitative biomarker, which proved effective in statistically differentiating pediatric patients with Acute Rheumatic Fever from healthy controls on our dataset. This reinforces the value of interpretable, classical computer vision methods as objective tools for clinical decision support in RHD.

As this is a work in progress, future efforts will focus on addressing the study's current limitations to build upon these preliminary findings. A key priority is to expand the validation of the proposed biomarker on larger, multi-center clinical cohorts to establish its generalizability. Furthermore, we plan to explore the use of deep learning models for the segmentation task and conduct a rigorous benchmark comparison between our classical pipeline and these neural network-based approaches to assess performance and interpretability trade-offs. To advance towards a fully operator-independent system, future work will also include the development of an automated module for Region of Interest detection and a detailed sensitivity analysis of the pipeline's parameters. These planned advancements are essential steps toward maturing this tool for potential clinical integration in RHD screening.

References

[1] G. A. Roth, C. Johnson, A. Abajobir, F. Abd-Allah, S. F. Abera, G. Abyu, M. Ahmed, B. Aksut, T. Alam, K. Alam, and et al., "Global, regional, and national burden of cardiovascular diseases for 10 causes, 1990 to 2015," *Journal of the American College of Cardiology*, vol. 70, no. 1, pp. 1–25, 2017.

[2] R. H. Webb, C. Grant, and A. Harnden, "Acute rheumatic fever," *BMJ*, vol. 351, p. h3443, 2015.

[3] M. T. B. C. Leal, L. S. A. Passos, F. V. Guarçoni, J. M. d. S. Aguiar, R. B. R. d. Silva, T. M. N. d. Paula, R. F. d. Santos, M. C. L. Nassif, N. F. Gomes, T. C. Tan *et al.*, "Rheumatic heart disease in the modern era: recent developments and current challenges," *Revista da Sociedade Brasileira de Medicina Tropical*, vol. 52, no. 00, p. e20180041, 2019.

[4] B. L. Silva, A. C. C. de Carvalho, A. V. S. Santos, V. B. P. Santos, A. C. O. Silva, A. P. S. Brandão, and B. E. X. de Albuquerque, "Internações e Óbitos por doença reumática do coração: Tendências epidemiológicas e impacto na saúde pública," *Brazilian Journal of Innovation in Health Science*, vol. 4, no. 1, pp. 1–9, 2024.

[5] C. M. Otto, R. A. Nishimura, R. O. Bonow, B. A. Carabello, J. P. Erwin, F. Gentile, H. Jneid, E. V. Krieger, M. Mack, C. McLeod, P. T. O'Gara, V. H. Rigolin, T. M. Sundt, A. Thompson, and C. Toly, "2020 acc/aha guideline for the management of patients with valvular heart disease: A report of the american college of cardiology/american heart association joint committee on clinical practice guidelines," *Journal of the American College of Cardiology*, vol. 77, no. 4, pp. e25–e197, 2021.

[6] R. Saxena, S. Mishra, N. Bhardwaj, R. Bansal, and R. Gupta, "The echocardiographic diagnosis of rheumatic heart disease: A comprehensive review," *Journal of the American College of Cardiology: Asia*, vol. 4, no. 4, pp. 681–683, 2024.

[7] S. Seitler, M. Zuhair, A. Shamsi, J. J. Bray, A. Wojtaszewska, A. Siddiqui, M. Ahmad, J. Fairley, R. Providencia, and A. Akhtar, "Cardiac imaging in rheumatic heart disease and future developments," *European Heart Journal Open*, vol. 3, no. 2, p. oeac060, 2023.

[8] G. F. Cacao, D. Du, and N. Nair, "Unsupervised image segmentation on 2d echocardiogram," *Algorithms*, vol. 17, no. 11, p. 515, 2024.

[9] M. Ploutz, J. C. Lu, J. Scheel, C. Webb, G. J. Ensing, T. Aliku, P. Lwabi, C. Sable, and A. Beaton, "Handheld echocardiographic screening for rheumatic heart disease by non-experts," *Heart*, vol. 102, no. 1, pp. 35–39, 2016.

[10] N. Otsu, "A threshold selection method from gray-level histograms," *IEEE Transactions on Systems, Man, and Cybernetics*, vol. 9, no. 1, pp. 62–66, 1979.

[11] G. Litjens, T. Kooi, B. E. Bejnordi, A. A. A. Setio, F. Ciompi, M. Ghafoorian, J. A. van der Laak, B. van Ginneken, and C. I. Sánchez, "A survey on deep learning in medical image analysis," *Medical Image Analysis*, vol. 42, pp. 60–88, 2017.

[12] J. S. Suri, K. Liu, S. Singh, S. N. Laxminarayan, X. Zeng, and L. Reden, "Shape recovery algorithms using level sets in 2-d/3-d medical imagery: a state-of-the-art review," *IEEE Transactions on information technology in biomedicine*, vol. 6, no. 1, pp. 8–28, 2002.

[13] A. Ghorbani, D. Ouyang, A. Abid, B. He, J. H. Chen, R. A. Harrington, D. H. Liang, E. A. Ashley, and J. Y. Zou, "Deep learning interpretation of echocardiograms," *NPJ digital medicine*, vol. 3, no. 1, pp. 1–8, 2020.

[14] C. Chen, C. Qin, H. Qiu, G. Tarroni, J. Duan, W. Bai, and D. Rueckert, "Deep learning for cardiac image segmentation: A review," *Frontiers in Cardiovascular Medicine*, vol. 7, p. 25, 2020.

[15] O. Ronneberger, P. Fischer, and T. Brox, "U-net: Convolutional networks for biomedical image segmentation," in *Medical image computing and computer-assisted intervention–MICCAI 2015: 18th international conference, Munich, Germany, October 5-9, 2015, proceedings, part III 18*. Springer, 2015, pp. 234–241.

[16] B. S. Andreassen, F. Veronesi, O. Gerard, A. H. S. Solberg, and E. Samset, "Mitral annulus segmentation using deep learning in 3-d transesophageal echocardiography," *IEEE journal of biomedical and health informatics*, vol. 24, no. 4, pp. 994–1003, 2019.

[17] K. Brown, P. Roshanitabrizi, J. Rwebembera, E. Okello, A. Beaton, M. G. Linguraru, and C. A. Sable, "Using artificial intelligence for rheumatic heart disease detection by echocardiography: Focus on mitral regurgitation," *Journal of the American Heart Association*, vol. 13, no. 2, p. e031257, 2024.

[18] M. Kass, A. Witkin, and D. Terzopoulos, "Snakes: Active contour models," *International journal of computer vision*, vol. 1, no. 4, pp. 321–331, 1988.

[19] P. Kulkarni and D. Madathil, "Echocardiography image segmentation using semi-automatic numerical optimisation method based on wavelet decomposition thresholding," *International Journal of Imaging Systems and Technology*, 2021.

[20] V. V. Danilov, I. P. Skirnevskiy, O. M. Gerget, E. E. Shelomentcev, D. Y. Kolpashchikov, and N. V. Vasilyev, "Efficient workflow for automatic segmentation of the right heart based on 2d echocardiography," *The International Journal of Cardiovascular Imaging*, vol. 34, pp. 1339–1352, 2018.

[21] G. d. F. Barros Filho, A. L. C. de Almeida, I. Solha, E. F. de Medeiros, A. d. S. Felix, J. C. de Lima Júnior, M. D. T. de Melo, and M. C. Rodrigues, "Medição automática de valva mitral a partir de ecocardiograma utilizando processamento digital de imagens," *Arquivos Brasileiros de Cardiologia: Imagem Cardiovascular*, vol. 36, p. e371, 2023.

[22] M. H. Gewitz, R. S. Baltimore, L. Y. Tani, C. A. Sable, S. T. Shulman, J. Carapetis, B. Remenyi, K. A. Taubert, A. F. Bolger, L. Beerman *et al.*, "Revision of the jones criteria for the diagnosis of acute rheumatic fever in the era of doppler echocardiography: a scientific statement from the american heart association," *Circulation*, vol. 131, no. 20, pp. 1806–1818, 2015.

[23] G. Bradski, "The opencv library," *Dr. Dobb's Journal of Software Tools*, vol. 25, no. 11, pp. 120–122, 2000.

[24] S. van der Walt and et al., "scikit-image: image processing in python," *PeerJ*, vol. 2, p. e453, 2014.

[25] R. C. Gonzalez and R. E. Woods, *Digital Image Processing*, 4th ed. Pearson, 2018.

[26] L. S. A. Passos, M. C. P. Nunes, and E. Aikawa, "Rheumatic heart valve disease pathophysiology and underlying mechanisms," *Frontiers in Cardiovascular Medicine*, vol. 7, 2021.